Write Up of Work and Experiments So Far

Henry

June 13, 2025

1 Surface Elevation and Flight Height

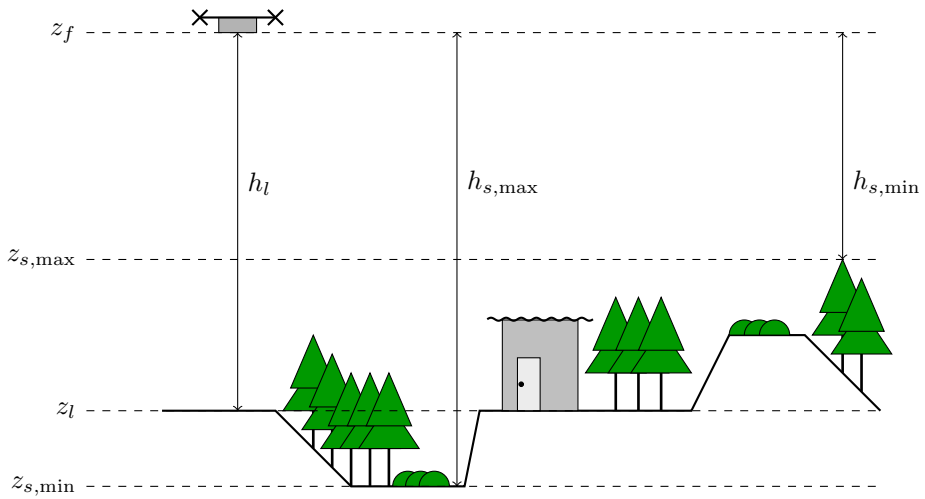

Figure 1: Schematic illustration of uneven terrain with ground features and flight height.

Figure 1 shows a terrain cross section over an area of interest (AOI), annotated with both absolute elevations (relative to the Australian Height Datum, AHD) and the corresponding UAV flight heights above ground.

In this schematic, the solid line depicts the true ground surface profile, including dips and peaks as captured by a Digital Elevation Model (DEM). The overlaid symbols for trees, shrubs, and the building represent above-ground features that together constitute a Digital Surface Model (DSM).

Absolute elevations denoted by z mark key points relative to the Australian Height Datum (AHD).

z_l: the elevation at the launch point.

z_f: the elevation of the UAV's sensor while in flight, assumed to be constant across AOI.

$z_{s,(x,y)}$: the elevation of the surface at point (x, y).

$z_{s,\min}$: the minimum surface elevation.

$z_{s,\max}$: the maximum surface elevation.

Heights denoted by h mark the relative distance between the UAV sensor and the surface.

$h_l = z_f - z_l$, is the flight height at take off. It generally the value given to a flight planner.

$h_{s,(x,y)} = z_f - z_{s,(x,y)}$, is the distance between the UAV and and surface point (x, y).

$h_{s,max} = z_f - z_{s,min}$, is the maximum distance between the UAV and the surface within the AOI.

$h_{s,min} = z_f - z_{s,max}$, is the minimum distance between the UAV and the surface within the AOI.

Symbol	Definition
z_l	Launch elevation (AHD)
$z_{s,\max}$	Maximum surface elevation (AHD)
$z_{s,\min}$	Minimum surface elevation (AHD)
z_f	Flight elevation (AHD)
$z_{s,(x,y)}$	Surface elevation at point (x, y) (AHD)
h_l	Flight height above launch ground
$h_{s,(x,y)}$	Flight height above surface at point (x, y)
$h_{s,\max}$	Height above highest terrain point
$h_{s,\min}$	Height above lowest terrain point

Table 1: Nomenclature of symbols used in this thesis.

2 Constraints

2.1 Pixel Resolution

The GSD acheived flying at $h_{s,(x,y)}$ is,

$$GSD_{(x,y)} = \frac{S_x}{f \cdot S_a} \cdot h_{s,(x,y)} [1] \tag{1}$$

$$h_{s,(x,y)} = \frac{GSD_{(x,y)} \cdot f \cdot S_a}{S_x} \tag{2}$$

$$= \frac{GSD_{(x,y)} \cdot f}{S_\delta} \tag{3}$$

To guareantee that the ground smapling distance at any point $GSD_{(x,y)}$ does not exceed the maximum alowable ground sampling distance GSD_{req}:

$$h_{s,max} \leq \frac{GSD_{req} \cdot f}{S_\delta} \tag{4}$$

$$z_f - z_{s,min} \leq \frac{GSD_{req} \cdot f}{S_\delta} \tag{5}$$

$$h_l + z_l - z_{s,min} \leq \frac{GSD_{req} \cdot f}{S_\delta} \tag{6}$$

$$h_l \leq \frac{GSD_{req} \cdot f}{S_\delta} + z_{s,min} - z_l \tag{7}$$

2.2 Diffraction Resolution

Diffraction preamble...

Given the diameter of the Airy disk projected to the surface at any point $d_{A,proj,(x,y)}$ must meet the minimum resolution requirement:

$$d_{A,proj,(x,y)} \leq GSD_{req} \tag{8}$$

$$d_A \cdot \frac{h_{s,(x,y)}}{f} \leq GSD_{req} \tag{9}$$

$$\frac{2.44 \cdot N \cdot \lambda \cdot h_{s,(x,y)}}{f} \leq GSD_{req} \tag{10}$$

$$h_{s,(x,y)} \leq \frac{GSD_{req} \cdot f}{2.44 \cdot N \cdot \lambda} \tag{11}$$

Again, to guareantee the Airy disk diameter does not exceed the GSD requirement at any point:

$$h_{s,max} \leq \frac{GSD_{req} \cdot f}{2.44 \cdot N \cdot \lambda} \tag{12}$$

$$z_f - z_{s,min} \leq \frac{GSD_{req} \cdot f}{2.44 \cdot N \cdot \lambda} \tag{13}$$

$$h_l + z_l - z_{s,min} \leq \frac{GSD_{req} \cdot f}{2.44 \cdot N \cdot \lambda} \tag{14}$$

$$h_l \leq \frac{GSD_{req} \cdot f}{2.44 \cdot N \cdot \lambda} + z_{s,min} - z_l \tag{15}$$

2.3 Depth of Field

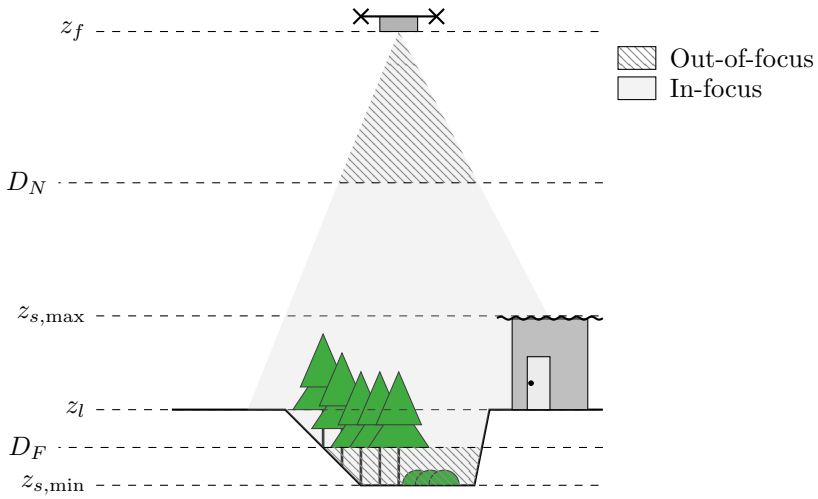

Figure 2: Near and far limits to a UAV mounted sensor's field of view. Shrubs at the bottom of the gully fall beyond the far limit and are thus considerd out of focus.

The near limit D_N and far limit D_F denote the distances along the optical axis from the sensor plane (or camera's principal plane) to the near and far focus limits, respectively.

$$D_N = \frac{s \cdot H}{H + s}[1] \tag{16}$$

$$D_F = \frac{s \cdot H}{H - s}[1] \tag{17}$$

$$\tag{18}$$

where s is the set focus distance and H is the Hyperfocal distance of the sensor:

$$H = \frac{f^2}{N \cdot c} + f[1] \tag{19}$$

While most imaging systems support adjustable focus distances, it is reasonable to assume a fixed focus distance for drone-based photogrammetry. In typical deployments, the camera is calibrated once prior to operation, and the focus is then locked. Recalibrating before every flight is inefficient and often impractical, particularly for fully autonomous systems. Maintaining a constant focus distance ensures that internal camera parameters, such as focal length and distortion coefficients, remain valid across missions, ensuring reliable and repeatable data capture without the need for continual recalibration [2].

Equation 17 indicates as s approaches H from below, D_F tends to infinity; if s exceeds H, the denominator becomes negative, yielding a non-physical negative far limit. To ensure a real, non-negative focus range, the focus distance must satisfy,

$$s \leq H \tag{20}$$

To ensure the entire surface is captured in focus by the sensor, launch height must be adjusted such that the minimum and maxium elevations fall within the near and far limits to the DOF.

$$D_N \leq z_f - z_{s,\max} \tag{21}$$

$$D_N \leq z_l + h_l - z_{s,\max} \tag{22}$$

$$h_l \geq D_N + z_{s,\max} - z_l \tag{23}$$

$$h_l \geq \frac{s \cdot H}{H + s} + z_{s,\max} - z_l \tag{24}$$

$$h_l \geq \frac{N \cdot c \cdot f \cdot s + s \cdot f^2}{N \cdot c \cdot (f + s) + f^2} + z_{s,\max} - z_l \tag{25}$$

$$D_F \geq z_f - z_{s,\min} \tag{26}$$

$$D_F \geq z_l + h_l - z_{s,\min} \tag{27}$$

$$h_l \leq D_F + z_{s,\min} - z_l \tag{28}$$

$$h_l \leq \frac{s \cdot H}{H - s} + z_{s,\min} - z_l \tag{29}$$

$$h_l \leq \frac{N \cdot c \cdot f \cdot s + s \cdot f^2}{N \cdot c \cdot (f - s) + f^2} + z_{s,\min} - z_l \tag{30}$$

Figure 2 shows a scene where launch height meets 25 but not 30 resulting in shrubery in the gully being captured out of focus.

2.4 Motion Blur

Motion blur preamble...

Motion blur δ meausred in pixels, can be estimated at any point (x, y) in the direction of flight as,

$$\delta = \frac{v_{(x,y)} \cdot I_t}{GSD_{(x,y)}} [3] \tag{31}$$

Assuming the linear velocity remains constant across the AOI, it must be selected such that motion blur is less than a given maximum $\delta_{\max}$ at all points.

$$v \leq \frac{GSD_{(x,y)} \cdot \delta_{\max}}{I_t} \tag{32}$$

Given,

$$GSD_{\min} = \frac{S_\delta}{f} \cdot h_{s,(\min)} \tag{33}$$

Velocity must be selected such that,

$$v \leq \frac{S_\delta \cdot h_{s,(\min)} \cdot \delta_{\max}}{f \cdot I_t} \tag{34}$$

$$v \leq \frac{S_\delta \cdot (z_f - z_{s,\max}) \cdot \delta_{\max}}{f \cdot I_t} \tag{35}$$

$$v \leq \frac{S_\delta \cdot (h_l + z_l - z_{s,\max}) \cdot \delta_{\max}}{f \cdot I_t} \tag{36}$$

or height must be selected such that,

$$h_l \geq \frac{v \cdot f \cdot I_t}{S_\delta \cdot \delta_{\max}} - z_l + z_{s,\max} \tag{37}$$

However, the selected exposure time I_t is tied to the required exposure value,

$$EV = \log_2(\frac{N^2}{I_t}) + \log_2(\frac{100}{ISO}) \tag{38}$$

and can thus be expressed in terms of aperture if we assume ISO is fixed at its maximum ($ISO_{\max}$),

$$I_t = \frac{100 \cdot N^2}{2^{EV} \cdot ISO_{\max}} \tag{39}$$

Hence,

$$h_l \geq \frac{100 \cdot N^2 \cdot v \cdot f}{2^{EV} \cdot ISO_{\max} \cdot S_\delta \cdot \delta_{\max}} - z_l + z_{s,\max} \tag{40}$$

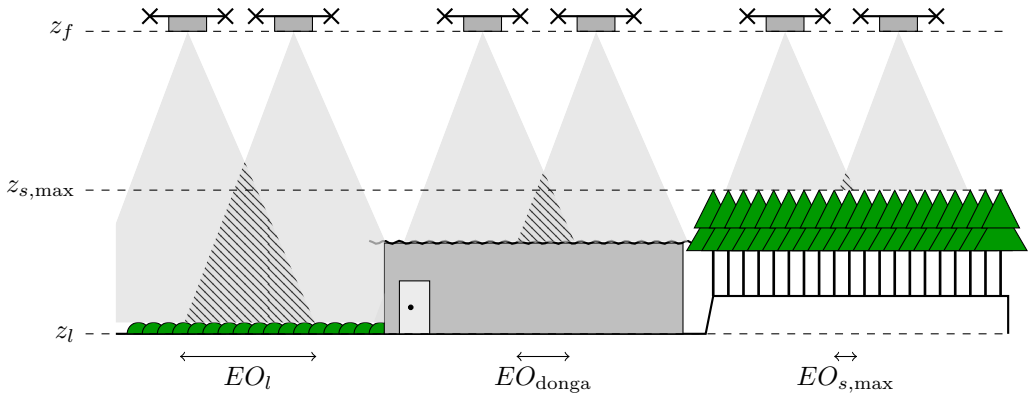

Figure 3: End overlaps at differnt surface hights. With a constant flight elevation, the end overlap $EO_{s,\max}$ when the surface elevation is at its maximum, is less than the overlap at launch EO_l.

2.5 End Overlap

Endlap preamble....
Given a minimum required percentage overlap between sucessive images EO_{req}, the neccasary ground spacing between image captures at any point $E_{(x,y)}$ is,

$$E_{(x,y)} = G_E \cdot (1 - \frac{EO_{req}}{100})[1] \tag{41}$$

where G_E is the ground field of view in the direction of flight. Assuming the sensor is orientated such that the y axis is paralell to the direction of flight[1],

$$E_{(x,y)} = \frac{S_y}{f} \cdot h_{s,(x,y)} \cdot (1 - \frac{EO_{req}}{100}) \tag{42}$$

As the minimum end overlap will occur at $h_{s,min}$ as illistrated in Figure 3,

$$E_{\max} = \frac{S_y}{f} \cdot h_{s,\min} \cdot (1 - \frac{EO_{req}}{100}) \tag{43}$$

$$= \frac{S_y}{f} \cdot (h_l + z_l - z_{s,max}) \cdot (1 - \frac{EO_{req}}{100}) \tag{44}$$

$$\tag{45}$$

Thus, velocity must be selected such that,

$$v \leq I_{f,\max} \cdot E_{\max} \tag{46}$$

$$v \leq I_{f,\max} \cdot \frac{S_y}{f} \cdot (h_l + z_l - z_{s,max}) \cdot (1 - \frac{EO_{req}}{100}) \tag{47}$$

[1]Orientating the wider x axis of the sensor perpendicular to the flight direction, increases the area covered by each flight line. This minimises flight time as less turns are required to cover the same area.

or height must be selected such that,

$$h_l \geq \frac{v \cdot f}{I_{f,\max} \cdot S_y \cdot (1 - \frac{EO_{req}}{100})} - z_l + z_{s,max} \tag{48}$$

where $I_{f,\max}$ is the maximum capture freqency of the imaging system.

2.6 Constant Constraints

Legal and Physical

3 Optimization

3.1 Objective

Objective preamble about coverage removing flight path from consideration etc...

The coverage rate can be defined as the area covered by the sensors field of view every second.

$$F(h, v) = \frac{S_x}{f} \cdot h \cdot v \tag{49}$$

3.2 Solution Space

Present the solution space for a few examples and explain why a optimiser is required.

3.3 Problem Formulation

Rather than attempting to search the full three-dimensional space (h, v, N) simultaneously, we can exploit the fact that sensor apertures are constrained to a discrete set of stops $\mathcal{N} = \{N_1, N_2, ..., N_n\}$. This means we can slice the 3D solution space into n 2D spaces and compare the optimal height and velocity for each $N \in \mathcal{N}$.

Thus, for a fixed aperture, each upper bound $u_i(v; N) \in \mathcal{U}$ and lower bound $l_j(v; N) \in \mathcal{L}$ on height derived in Section 2 is affine in (v, h),

$$h \leq m_i(N)v + b_i(N) \quad \forall i \in \mathcal{U} \tag{50}$$
$$h \geq \bar{m_j}(N)v + \bar{b_j}(N) \quad \forall j \in \mathcal{L} \tag{51}$$

As each upper bound is linear, their pointwise minimum,

$$h_{\max}(v; N) = \min_{i \in \mathcal{U}} \{m_i(N)v + b_i(N)\} \tag{52}$$

is a concave piecewise linear surface in the (v, h) plane. A feasible (v, h) must lie at or below this surface. Similarly, all feasible (v, h) must lie at or above the convex peicewise linear surface of linear lower bounds,

$$h_{\min}(v; N) = \max_{j \in \mathcal{L}} \{\bar{m_j}(N)v + \bar{b_j}(N)\} \tag{53}$$

As the objective function 49 is monotonically increasing in h, the optimal height at a fixed velocity and aperture will always lie on the upper bound. That is,

$$h(v; N)^* = h_{\max}(v; N), \quad \forall\, v \in [v_{\min}, v_{\max}] \tag{54}$$

This collapses the problem into a one dimentional optimisation over velocity,

$$\max_{v \in [v_{\min}, v_{\max}]} F(v; N) \tag{55}$$

where,

$$F(v; N) = \frac{S_x}{f} \cdot h_{\max}(v, N) \cdot v \tag{56}$$

3.4 Vertex Enumeration Justification

Within a given segment I_i the objective 56 becomes quadratic,

$$F(v;N) = \frac{S_x}{f}(m_i(N)v^2 + b_i(N)v) \tag{57}$$

and the local maximum can only occur at two points.

1. If $m_i(N) \geq 0$, $F(v;N)$ is linear or stricly convex in v. In both cases the local maximum occurs at the right end point of the segment.

2. If $m_i(N) < 0$, $F(v;N)$ is stricly concave and a local maximum can occur at the stationary point where $\frac{\partial F}{\partial v} = 0$,

$$\hat{v_i} = -\frac{b_i(N)}{2\,m_i(N)} \tag{58}$$

   which, provided it lies inside I_i and satisfies the floor constraint, is a local maximum. If $\hat{v_i}$ is infeasible or outside the segment, again the right endpoint is best.

Hence, the global maximiser of the one-dimensional problem 55 must occur at a breakpoint of $h_{\max}(v;N)$, at the domain endpoints or, in the case that $m_i(N) < 0$, at a stationary point $\hat{v_i}$.

However, the upper bounds derived in Section 2 are constant in (v,h). Therefore all $m_i(N) = 0$, the objective function 56 is linear in v and we can ignore the stationary point $\hat{v_i}$.

This follows the fundemental theorem in linear optimisation; if a linear program has an optimal solution, then at least one optimal solution occurs at a vertex (an extreme point) of its feasible polytope [4]. In our setting the "polytope" in the (v,h) plane is defined by the peicewise linear functions, $h_{\max}(v;N)$ and $h_{\min}(v;N)$.

By restricting our search to this finite set of velocities, we avoid any need for iterative solvers or numerical gradients. The method is both *exact* (no risk of local optima) and *efficient* (only n evaluations for n breakpoints), compared with a generic LP or nonlinear solver that would introduce unnecessary overhead or reliance on convergence tolerances.

3.5 Vertex Enumeration Algorithm

To identify the true breakpoints of the concave envelope $h_{\max}(v;N)$, we start by computing two candidate sets:

$$\mathcal{I}_{u,u} = \left\{ v \in [v_{\min}, v_{\max}] \;\middle|\; \exists\, i,k \in \mathcal{U},\ i<k:\ u_i(v;N) = u_k(v;N) \right\} \tag{59}$$

and

$$\mathcal{I}_{u,\ell} = \left\{ v \in [v_{\min}, v_{\max}] \;\middle|\; \exists\, i \in \mathcal{U},\ \exists\, j \in \mathcal{L}:\ u_i(v;N) = \ell_j(v;N) \right\} \tag{60}$$

However, not every intersection in these sets is a genuine vertex of the feasible ploytope:

- Redundant kinks: if the same segment of $h_{\max}(v;N)$ remains active immediately before and after the intersection, v is not an endpoint of the segment and cannot be a local maximum.

- Infeasible points: if at v the active ceiling lies below the floor ($h_{\max}(v;N) < h_{\min}(v;N)$), no valid flight height exists at this velocity.

We therefore prune from $\mathcal{I}_{u,u} \cup \mathcal{I}_{u,\ell}$, any velocity satisfying either condition. Finally, we add back the domain endpoints $v_{\min}$ and $v_{\max}$ (if they are feasible). The resulting set of velocities $\mathcal{V}(N)$ will contain the optimal velocity for a given aperture.

For each aperture N in our discrete set $\mathcal{N}$, we then evaluate the objective function

$$F(v; N) \;=\; \frac{S_x}{f}\, v\, h_{\max}(v; N), \quad \forall\, v \in \mathcal{V}(N) \tag{61}$$

and record the parameters (v, h) yielding the largest $F(v; N)$. Once we have done this for every aperture, we compare the best rates $\{F^*(N) \mid N \in \mathcal{N}\}$ and select the aperture N^* with the highest mapping speed. The corresponding configuration

$$\left(v^*, h^*, N^*\right) \tag{62}$$

is guaranteed to be the global optimum.

3.6 Variables and Constants

3.6.1 Decision Variables

- Flight Height (h) is the distance from the sensor plane to the ground at take off. Assumed to be constant throughout the flight unless terrian following enabled using a DEM or laser. Terrain following is recomended for areas with large changes in elevation that register on a DEM.
- Velocity (v) is the linear velocity of the UAV in reference to the ground while capturing data.
- Aperture (N) is denoted as an f value that meausres the light gathering ability of an optical system. It is the ratio of the focal length (f) and diameter of the entrance pupil (D) ($N = \frac{f}{D}$).
- Film Speed (ISO) is a measure of the digital sensor's sensitivity to light.
- Exposure Time (I_t) is the period of time a sensor is exposed to light. It is the inverse of shutter speed and often refered to interchangably.

3.6.2 Quality Requirements

- Ground Sampling Distance (GSD) is a measure of spatial resolution in an image. Ecenssially it represents the smallest resolvable area in an image. In remote sensing it refers to the distance between centres of adjacent pixels projected onto the ground.
- Motion Blur (δ) is the change in scene during a single sensor exposure generally denoted as a percentage of pixel pitch. Motion blur of 100% indicates information from one GSD will be spread across two pixels rather than one in the direction of motion.
- Side Overlap (SO) is the proportion images from adjacent flight lines overlap.
- End Overlap (EO) is the proortion images overlap in the direction of flight.
- Exposure Value (EV) is a measure of equivelant combinations of Aperture, ISO, and Exposure Time.

3.6.3 Lens Characteristics

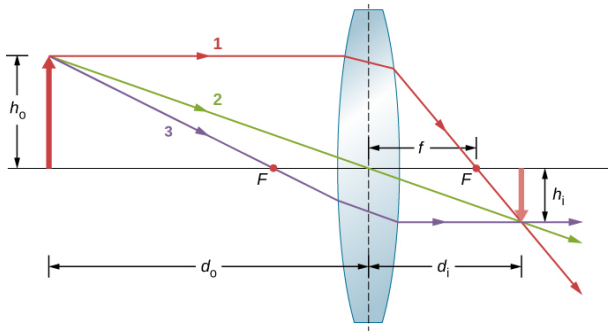

Figure 4: Ray tracing is used to locate the image formed by a lens. Rays originating from the same point on the object are traced—the three chosen rays each follow one of the rules for ray tracing, so that their paths are easy to determine. The image is located at the point where the rays cross.

The focal point is the point on the optical axis at which all paralell rays intercect after passing through the lens. The distance from the principle plane of a lens to this point is the focal distance (f). Depending on the lens type, focal length can be imutable or mutable (zoom lens). The object distance (d_o) is the distance from the centre of a lens to the object of interest. Image distance (d_i) is the distance from a len's principal plane to the intersection of rays originating from the same point on the object of interest depicted in Figure 4. Under the thin lens approximation, a sharp image requires:

$$\frac{1}{f} = \frac{1}{d_o} + \frac{1}{d_i} \tag{63}$$

Thus, focus distance (s) is set by adjusting the distance between the principle plane of a lens and the sensor such that it is equal to the image distance when $d_o = s$ and the captured image is in focus.

- Focal Length (f) is the distance from the centre of a lens to the point at which paralell rays passing through the lens intersect, assuming lens thickness is negligible compared to its redius of curvature. It is often denoted in lens specifications as a 35mm equivelant focal length to allow comparison between cameras, however the following refers to the effective physical measurement.
- Focus Distance (s) is the distance from the lens to an object at which all paraxial rays [2] from that object converge at a single point on the image plane, ignoring lens aberations. Whilst most imaging systems have adjustable focus distance, we assume it remians fixed to avoid recalibration required for acurate postprcessing [3].

3.7 Sensor Characteristics

- Sensor Height (S_y) is the dimension of the sensor in the y direction.
- Sensor Width (S_x) is the dimension of the sensor in the x direction.
- Pixel pitch (S_δ) is the distance between the centres of adjacent pixels. Pixels are assumed to be aproximatly square in shape.
- Maximum Trigger Frequency (I_f^{max}) is the maximum number of photos that can be captured per second.

3.7.1 UAV Characteristics

- Maximum UAV Velocity (v_{UAV}^{max}) is the maximum linear velocity of the UAV assuming no wind.
- Minimum UAV Velocity (v_{UAV}^{min}) is the minium linear velocity of the UAV assuming no wind. For multi-rotor drones this is usually $0ms^{-1}$ as they can hover in place, however many fixed wing UAVs have minimum velocitys that place significant restrictions on their ability to meet end overlap and blur constraints.
- Maximum UAV Flight Height (h_{UAV}^{max}) is the maximum flight height set by the UAV manufacturer.
- Minimum UAV Flight Height (h_{UAV}^{min}) is the minimum flight height set by the UAV manufacturer.

[2] Paraxial rays are those that remain close to the optical axis and satisfy small-angle approximations
[3] SFM requires an acurate model of the camera to estimate pose

3.7.2 AOI Characteristics

- Maximum Surface Elevation ($z^{max}_{surface}$) is the highest point in the area of interest including surface features measured from the Australian Height Datum (AHD).
- Minimum Surface Elevation ($z^{min}_{surface}$) is the lowest point in the area of interest including surface features measured from the AHD.
- Launch Elevation (z_{launch}) is the altitude of the ground where the UAV is launched measured from the AHD.
- Legal Velocity Limit (v^{max}_{legal}) is the maxium UAV velocity set by the aviation laws in the area of interest.
- Legal Flight Ceiling (h^{max}_{legal}) is the maxium UAV flight height set by the aviation laws in the area of interest.
- Legal Flight Floor (h^{min}_{legal}) is the minimum UAV flight height set by the aviation laws in the area of interest.

3.8 Constraints

3.8.1 Height

Fixed:

$$h \leq h_{legal}^{max} \tag{64}$$
$$h \leq h_{UAV}^{max} \tag{65}$$
$$h \geq h_{legal}^{min} \tag{66}$$
$$h \geq h_{UAV}^{min} \tag{67}$$

Sensor Resolution (assuming flat ground):

$$h \leq \frac{GSD \cdot f}{S_\delta} \tag{68}$$

Sensor Resolution:

$$h \leq \frac{GSD \cdot f}{S_\delta} + (z_{surface}^{min} - z_{launch}) \tag{69}$$

Diffraction Resolution (assuming flat ground):

$$h \leq \frac{GSD \cdot f}{2.44 \cdot \lambda \cdot N} \tag{70}$$

Diffraction Resolution:

$$h \leq \frac{GSD \cdot f}{2.44 \cdot \lambda \cdot N} + (z_{surface}^{min} - z_{launch}) \tag{71}$$

Depth of Field Far Limit:

$$h \leq \frac{N \cdot c \cdot f \cdot s + s \cdot f^2}{N \cdot c \cdot (f - s) + f^2} - (z_{launch} - z_{surface}^{min}) \tag{72}$$

Depth of Field Near Limit:

$$h \geq \frac{N \cdot c \cdot f \cdot s + s \cdot f^2}{N \cdot c \cdot (f + s) + f^2} + (z_{surface}^{max} - z_{launch}) \tag{73}$$

Clear of ground:

$$h \geq z_{surface}^{max} - z_{launch} \tag{74}$$

3.8.2 Velocity

Fixed:

$$v \leq v_{legal}^{max} \tag{75}$$
$$v \leq v_{UAV}^{max} \tag{76}$$
$$v \geq v_{UAV}^{min} \tag{77}$$

Blur (assuming flat ground):

$$v \leq \frac{GSD \cdot \delta}{I_t} \tag{78}$$

End Overlap (assuming flat ground):

$$v \leq h \cdot I_f^{max} \cdot \frac{S_y}{f} \cdot (1 - \frac{EO}{100}) \tag{79}$$

3.8.3 Exposure

$$\log_2(\frac{N^2}{I_t}) + \log_2(\frac{100}{ISO}) = EV \tag{80}$$

References

[1] L. Roth, A. Hund, and H. Aasen, "PhenoFly Planning Tool: Flight planning for high-resolution optical remote sensing with unmanned areal systems," *Plant Methods*, vol. 14, no. 1, p. 116, Dec. 2018.

[2] T. Luhmann, C. Fraser, and H.-G. Maas, "Sensor modelling and camera calibration for close-range photogrammetry," *ISPRS Journal of Photogrammetry and Remote Sensing*, vol. 115, pp. 37–46, May 2016.

[3] J. O'Connor, M. J. Smith, and M. R. James, "Cameras and settings for aerial surveys in the geosciences: Optimising image data," *Progress in Physical Geography: Earth and Environment*, vol. 41, no. 3, pp. 325–344, Jun. 2017.

[4] D. Bertsimas and J. N. Tsitsiklis, *Introduction to Linear Optimization*, ser. Athena Scientific Series in Optimization and Neural Computation. Belmont, Mass: Athena Scientific, 1997.